

Biosensor as a Reaction-Diffusion System

Surya K. Ghosh, Tapanendu Kundu, Anirban Sain

Department of Physics, Indian Institute of Technology, Bombay, Powai, Mumbai-400 076, India.

We model a biosensor as a reaction-diffusion process in a confined geometry. When a solution containing unknown concentration of antigens are injected into the closed chamber of the sensor, the antigens diffuse and react with a functionalised surface. These surface reactions are then converted to an optical signal, the intensity of which indicates the level of antigen content in the solution. We probe the spatio-temporal behavior of the system by studying the governing equations, using mean field approximation and numerical integration. Mean field analysis gives important insights about the dynamics, but in order to compare with real experiments and extract the values of the relevant kinetic parameters, numerical integration was necessary. We track down the operating conditions for quick and efficient response of the sensor.

PACS numbers:

INTRODUCTION

Biosensor is an analytical device which can detect very small traces of specific bio-chemicals present in a carrier medium. It is used to detect, for example, *E. coli* in drinking water[1], hepatitis B surface antigen present in human serum[2] or pollutants in air[3]. The last decade has seen proliferation of such biosensors [4–6] in day to day use, mainly due to their, (a) quick response time[7], (b) sensitivity to minute amount of biomolecules[1], and (c) compactness and easy portability of the device. With these requirements in mind we model the functioning of a biosensor as a reaction diffusion system in a confined geometry. Using analysis, experimental data [8] and numerical solutions we obtain important insights about the temporal response of a particular sensor and identify the working conditions for which features (a) and (b) are strengthened.

The particular type of biosensors we focus on here are optics based chemical sensors which converts chemical reactions between biomolecules into optical signal which is then efficiently detected using fiber-optics technology. These fiber-optic biosensors are widely used for food safety and security applications [9]. In fiber-optic biosensors antibodies are immobilised on the surface of an optical fiber through which light is passed. The fiber is kept coaxially inside a cylindrical chamber and fluid containing the antigens(analytes) is injected into this chamber. Fig.1 shows schematic diagram of such a cylindrical fiber optic biosensor. Antigens bind to the antibody on the surface of the fiber and absorb evanescent waves generated by the light carrying fiber. This results in loss of intensity carried by the fiber. The evanescent wave absorbance(A) is given [10] by the following relation $A = \log \frac{P(0)}{P(L)}$ where $P(0)$ and $P(L)$ are power transmitted through the optical fiber (of length L) in the absence and presence of the absorbing medium respectively. Using the above formula, absorbance(A) can be expressed [10] in terms of the parameters of the system as $A \propto \left(\frac{L\lambda\epsilon}{R_i\delta N_A}\right)\sigma$ where λ is the wavelength of the light passing through optical fiber, ϵ is the extinction coefficient of the absorbing medium, δ is the typical size of the antigen-antibody complex, N_A is the numerical

aperture of the fiber, R_i is its radius and σ is the number of antigens bound per unit surface area of the fiber. The proportionality between A and σ allows us to connect experiment, where absorbance is measured, to our theory where surface density of bound antigens are calculated.

For this system we write down the governing reaction diffusion equations [11] and focus on the time dependence of the surface density of the bound antigens $\sigma(t)$. Typically the equations are analysed in the mean field limit with high bulk concentration of antigens in the medium. This produce rapid exhaustion of binding sites resulting in exponential saturation of the absorbance signal like the charging of a capacitor. But in practical use often the antigen concentration is relatively small compared to the antibody available on the fiber. We show that by taking advantage of fast diffusion one can still employ mean field approximation for the unbound antigen density in the bulk but now with a time dependent bulk concentration which decreases in time as antigen gradually binds to the antibody. In particular the antigen concentration in the bulk is expressed in terms of the total injected amount of antigen minus the bound amount. We show that distinctly different temporal saturation profile results in such cases which follows a hyperbolic tangent function.

This paper is organised as follows. We first introduce the geometry of the sensor and the equations governing the basic chemical kinetics of the system. Next we introduce a mean field approximation of the equations and point out its regime of validity. Then we numerically solve the coupled, nonlinear, dynamic equations and extract the values of the kinetic coefficients, relevant for our particular sensor, by comparing our numerical results with the experiment data. This gives an idea about the values of the kinetic coefficients, essential for characterising the dynamics of any such physio-chemical system. Thereafter our discussion is focused on the temporal response and saturation characteristics of the system. This allows us to partially answer the questions, when the antigen density is low, (a) how can we maximize the absorbance (i.e., bound surface density $\sigma(t)$) so that hardly any antigens are left in the bulk, and (b) how can we minimize the time taken to reach a given level of absorbance?

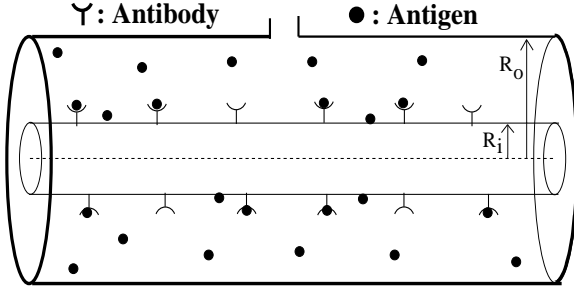


FIG. 1: Schematic diagram of a cylindrical biosensor.

MODEL

A cylindrical biosensor consists of an optical fiber of radius(R_i) kept coaxially in the middle of a closed cylinder of radius(R_o). Antibodies are immobilised on the optical fiber surface (at R_i) of length(L) and the solution in which antigens are injected, is kept inside the annular region of the cylinder (see fig.1). Analytes diffuse in the annular region (with diffusion constant D) and when an antigen comes close to an antibody, on the fiber surface, a specific (antigen-antibody) reaction occurs. Here an antigen molecule can bind to an antibody (with rate ω_b) and can also unbind (with rate ω_u) from the antibody with a much lower rate than binding. The values of the kinetic coefficients ω_b and ω_u are unknown a priori. The bulk concentration of antigens in the annular region is ρ and the concentration in the vicinity of the optical fiber surface is ρ_s . The surface concentration of bound antigens on the fiber are σ . Total number of injected antigen molecules N_0 can be represented by an equivalent bulk concentration $\rho_0 = N_0/V_0$, where $V_0 = \pi(R_o^2 - R_i^2)L$ is the volume of the cylindrical annular space. The surface concentration of immobilized antibody on the fiber surface is σ_0 . Therefore σ_0 set the maxima for σ . All the bulk and surface concentrations are expressed in units of number per unit volume and number per unit area respectively. The area of the optical fiber surface on which reaction can occur is $A_0 = 2\pi R_i L$. Now we present the dynamical equations describing the above processes. For the time being we will discuss the specific reactions only. The bulk density changes as

$$\frac{d\rho}{dt} = D\nabla^2\rho - \delta(r - R_i)[\rho(\sigma_0 - \sigma)\omega_b - \omega_u\sigma] \quad (1)$$

where $\rho = \rho(r, \phi, z, t)$ is the spatio-temporal density of the antigen, with $R_o > r > R_i$ and $\rho_s = \rho(r \sim R_i, \phi, z, t)$ is the antigen concentration in the vicinity of the fiber surface. The first term on the right hand side represents bulk diffusion with a diffusion constant D and the second term represents surface reactions at the optical fiber surface ($r = R_i$). The first term in square bracket describes specific binding reactions which has been assumed to be of 1st order in both bulk density of antigens and surface density of available antibodies. The second term represents 1st order, specific unbinding reactions.

The corresponding change in the concentration of the surface bound antigens is given by

$$\frac{d\sigma}{dt} = \rho_s(\sigma_0 - \sigma)\omega_b - \omega_u\sigma. \quad (2)$$

Here $\sigma = \sigma(\phi, z, t)$ is the spatio-temporal surface concentration of antibody-antigen pairs and σ_0 is the uniform surface concentration of antibody on the optical fiber surface. These equations can be nondimensionalized. Towards that, we rescale the bulk and the surface densities as $\tilde{\rho} = \frac{\rho}{\rho_0}$, $\tilde{\rho}_s = \frac{\rho_s}{\rho_0}$ and $\tilde{\sigma} = \frac{\sigma}{\sigma_0}$; the space and time variables as $\tilde{r} = r/R_i$, $\tilde{z} = z/L$ and $\tilde{t} = \frac{tD}{R_i^2}$. In terms of the resulting dimensionless kinetic coefficients $\tilde{\omega}_b = \omega_b\beta$, $\tilde{\omega}_u = \frac{\omega_u}{\rho_0}\beta$, where $\beta = \frac{R_o^2}{D}\rho_0$, the equations of motion read,

$$\frac{d\tilde{\rho}}{d\tilde{t}} = \tilde{\nabla}^2\tilde{\rho} - \delta(\tilde{r} - 1) \left(\frac{\sigma_0}{\rho_0 R_i} \right) [\tilde{\rho}(1 - \tilde{\sigma})\tilde{\omega}_b - \tilde{\omega}_u\tilde{\sigma}] \quad (3)$$

$$\frac{d\tilde{\sigma}}{d\tilde{t}} = \tilde{\rho}_s(1 - \tilde{\sigma})\tilde{\omega}_b - \tilde{\omega}_u\tilde{\sigma} \quad (4)$$

Here $\frac{\sigma_0}{\rho_0 R_i}$ is a dimensionless parameter.

In the particular system of our interest here, GaHIgG and HIgG molecules are used as antibody and antigen, respectively. The antibodies(GaHIgG) are pasted on the optical fiber surface and an uniform solution of antigen(HIgG) is injected into the annular region of the cylindrical biosensor. In previous work [8] the optimum geometric parameters of the system, namely, radius of the fiber R_i , outer radius of the chamber R_o and length of the fiber L have been identified to be 0.1mm, 1mm and 5cm, respectively.

Let the total number of immobilised antibodies on the optical fiber surface be N_s and the number of bound antigens on the optical fiber surface, forming antigen-antibody pairs, be $N_\sigma(t)$. Thus the corresponding surface concentrations are $\sigma_0 = N_s/A_0$ and $\sigma = N_\sigma(t)/A_0$. We assume that absorbance(A) is proportional to the number of bound antigen-antibody pairs $N_\sigma(t)$. The antibody-antigen surface reaction creates a depletion in the antigen concentration ρ near the fiber surface, compared to that in the bulk. This density difference activates diffusion of antigens towards the optical fiber surface, from the bulk. Subsequently more surface bindings occur and number of unbound antibodies left on the surface $N_s - N_\sigma(t)$ goes down in time. This process goes on till a dynamic equilibrium is reached near the optical fiber surface and the diffusion stops as ρ_s becomes equal to ρ .

We now aim to understand, a) which factors control the response time, in particular what is the characteristic saturation time for the signal (the absorbance A), and b) What is the optimum amount of antibody, needed for an efficient detection. Answers to these questions are nontrivial. In principle, saturation in the absorbance signal can be attained in two ways. First, if antigen density is low compared to available absorbance sites i.e., $N_0 \ll N_s$, then we expect $\sigma_{max} \leq N_0/A_0$. Second, in the opposite limit, $N_0 \gg N_s$, we expect $\sigma_{max} \leq N_s/A_0$, i.e., antigens exhausting all the

available binding sites on the fiber. But in reality, σ_{max} could be much lesser than the above theoretical limits because depending on the reaction rates ω_b and ω_u , there could be a substantial amount of antigen left in the vicinity of the fiber, maintaining a dynamic equilibrium between binding and unbinding events. For the first case, when antigens are few, the efficiency of the sensor will be severely compromised if a substantial fraction of antigens stay back in the bulk. This leads us to a detailed study of the evolution of $\sigma(t)$. We do this first, by using a mean field approximation and then by solving Eq.3-4 numerically. But in order to answer questions 'a' and 'b' quantitatively, we first need to estimate the microscopic kinetic coefficients for the system. We do this by fitting our numerical solution to the experimental data[8].

MEAN FIELD ANALYSIS

Total number of antigen initially injected into the liquid be N_0 so the initial concentration is $\rho_0 = \frac{N_0}{V_0}$ where $V_0 (= \pi(R_o^2 - R_i^2)L)$ is the volume of the annular region. At initial time all the antigen molecules (N_0) are in the annular volume and there are no antigen molecules bound on the surface of the optical fiber. As the surface reaction starts the number of antigen molecule on the surface, $N_\sigma(t)$ increases and conservation law dictates that the number of antigen molecules in the volume, $N_\rho(t)$ decreases.

In mean field approximation(MFA) we consider the surface concentration to be uniform over the whole optical fiber surface and the volume concentration to be uniform through out the annular volume of the chamber. Starting with $N_0 = \rho_0 V_0$ at $t = 0$, the antibody gets distributed between the bulk and the surface at later times. For $t > 0$, $N_0 = N_\rho(t) + N_\sigma(t) = \rho V_0 + \sigma A_0$. After extracting ρ and writing in a nondimensional form we have

$$\tilde{\rho} = 1 - \alpha \tilde{\sigma}, \quad (5)$$

where $\alpha = \frac{\sigma_0 A_0}{\rho_0 V_0} = \frac{N_s}{N_0}$. The bulk density being homogeneous and slaved by σ (via Eq.5) we need to consider only the equation of motion for the surface reaction, namely Eq.4. Substituting for ρ , from Eq.5, into Eq.4, and simplifying, we get

$$\frac{d\tilde{\sigma}}{d\tau} = \lambda_1 \tilde{\sigma}^2 - \lambda_2 \tilde{\sigma} + \lambda_3, \quad (6)$$

where $\lambda_1 = \alpha \tilde{\omega}_b$, $\lambda_2 = [(1 + \alpha)\tilde{\omega}_b + \tilde{\omega}_u]$ and $\lambda_3 = \tilde{\omega}_b$.

Integrating this Equation we get

$$\begin{aligned} \tau &= \int_{\tilde{\sigma}(0)=0}^{\tilde{\sigma}(\tau)} \left[\frac{d\sigma}{\lambda_1 \sigma^2 - \lambda_2 \sigma + \lambda_3} \right] \quad (7) \\ &= \frac{2}{i\lambda_R} \left[\tan^{-1} \left(\frac{\lambda_2}{i\lambda_R} \right) - \tan^{-1} \left(\frac{\lambda_2 - 2\lambda_1 \sigma}{i\lambda_R} \right) \right] \quad (8) \end{aligned}$$

where $\lambda_R = \sqrt{\lambda_2^2 - 4\lambda_1 \lambda_3}$. Inverting the above equation finally we arrive at the expression for σ as a function of the

scaled time (τ). In Fig.2 we compare this formula with the result obtained through numerical integration of Eq.3 and 4.

$$\tilde{\sigma}(\tau) = \frac{1}{2\lambda_1} \left[\lambda_2 - \lambda_R \tanh \left[\tanh^{-1} \left(\frac{\lambda_2}{\lambda_R} \right) + \frac{\lambda_R \tau}{2} \right] \right] \quad (9)$$

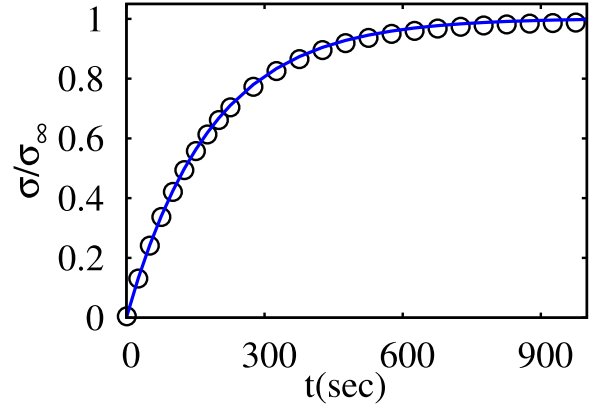


FIG. 2: Surface density of absorbed antigens $\sigma(t)$ versus time(t) in sec, y-axis is scaled with the saturation value of $\sigma(t)$, $\sigma_\infty = \sigma(t \rightarrow \infty)$. The symbols here are simulation data which matches exactly with the solid line, obtained from the mean field analysis. Both simulation and mean field analysis were done in the regime of fast diffusion with $\rho_0 = 0.1mg/ml$.

Further, in the steady state (denoted by subscript ' ∞ '),

$$\frac{d\tilde{\sigma}_\infty}{d\tau} = 0 = \lambda_1 \tilde{\sigma}_\infty^2 - \lambda_2 \tilde{\sigma}_\infty + \lambda_3$$

solving which we get

$$\tilde{\sigma}_\infty = \frac{\lambda_2 \pm \sqrt{\lambda_2^2 - 4\lambda_1 \lambda_3}}{2\lambda_1} = \frac{1}{2\lambda_1} [\lambda_2 \pm \lambda_R] \quad (10)$$

The minus sign corresponds to the physically acceptable solution as can be checked from the $\tau \rightarrow \infty$ limit of Eq.9.

The mean field approximation is likely to fail if diffusion is not sufficiently fast compared to the time scale at which surface binding reactions cause a depletion in the antigen concentration (ρ). In such a scenario the spatial inhomogeneity in ρ (along r) takes a long time, comparable to the saturation time of the sensor, to homogenise. A better understanding can be gained by comparing the time scales of the three processes: diffusion (t_D), binding (t_b) and unbinding (t_u). We get the individual time scales from eq.1, by comparing each term on the right hand side with the left hand side. For example, $\dot{\rho} \sim D\nabla^2 \rho$ gives, by dimensional analysis, $t_D^{-1} \sim \frac{D}{R^2}$. Similarly, $t_b^{-1} \sim \frac{\sigma_0 \omega_b}{R}$ and $t_u^{-1} \sim \frac{\sigma_0 \omega_u}{\rho_0 R}$. Here we have assumed $R = R_o - R_i$ to be the only relevant length scale. For diffusion, this is the spatial scale of density inhomogeneity. Now, t_b and t_u are the time scales over which density inhomogeneity are created near the fiber due to the surface reactions, while t_D is the time interval during which such inhomogeneities are ironed out. Therefore, mean field

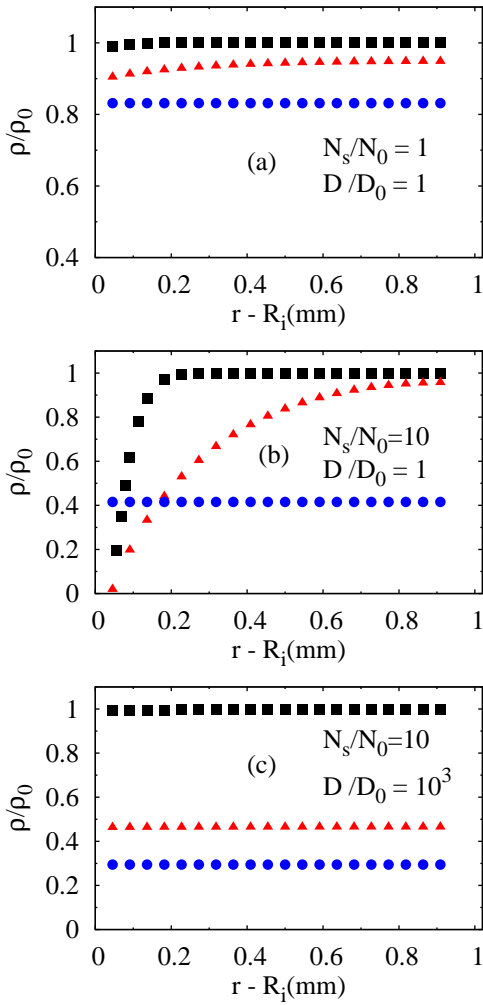


FIG. 3: Radial density profile ρ as a function of $r - R_i$, at three different times: right after start (square), at saturation (circle) and some intermediate time (triangle). a,b,c differ in parameters D and N_s/N_0 (which is proportional to σ_0 at fixed ρ_0). The diffusion constant $D_0 = 1.2 \times 10^5 \text{ cm}^2/\text{sec}$ is obtained through Fig.4. Transition from mean field to non-mean field type density profile occurs as we go from (a) to (b) by increasing N_s/N_0 . The reverse occurs as we go from (b) to (c) by increasing D . But note that, at a fixed ρ_0 , the fraction of antigens remaining in the bulk can be reduced (consequently the bound proportion can be increased) by increasing N_s/N_0 . This is desirable for making the sensor more sensitive, specially when ρ_0 is small. Values of ω_b and ω_u are same as those found through Fig.4 (to be discussed later).

approximation requires diffusion to be a faster process, i.e., $t_D \ll t_b, t_u$. These inequalities yield the criteria $\frac{\sigma_0 \omega_b R}{D} \ll 1$ and $\frac{\sigma_0 \omega_u R}{\rho_0 D} \ll 1$. The first inequality suggests that mean field approximation will be correct at high D or low σ_0 values. These conditions are verified in Fig.3. In the figure (where $N_s/N_0 \propto \sigma_0/\rho_0$) mean field theory is valid for the parameters in Fig.3a, but when N_s (equivalently σ_0) is hiked ten times (Fig.3b) it breaks down creating inhomogeneous $\rho(r)$. But now when D is hiked (Fig.3c) mean field homogeneous

solutions are recovered. The second inequality suggests, along with high D and low σ_0 , we also need low ρ_0 . Then only both $t_b, t_u \gg t_D$ can be satisfied. We have also verified this condition on ρ_0 along with similar conditions on ω_b and ω_u resulting from the inequalities.

NUMERICAL SOLUTION

We solve Eq.3-4, numerically, using cylindrical polar coordinate system (r, ϕ, z) . Uniform binning is used along z and ϕ ; while r coordinate is binned non uniformly such that the volume of each bin ($rdrd\phi dz$) is constant. Reflecting boundary condition is used at the walls of the cylindrical chamber, by ensuring zero currents at the boundaries. This is implemented by considering extra dummy bins at the boundaries. We fit the results to two different sets of experimental data[8] on $\sigma(t)$ versus t . These data sets were obtained at two widely different antigen densities, $\rho_0 = 0.001$ and 0.1 mg/ml , keeping all other experimental inputs same. Note that the non dimensional equations 3-4 do not explicitly scale with antigen density ρ_0 and therefore these data sets at different densities, $\rho_0 = 0.001, 0.1 \text{ mg/ml}$, can be treated as independent.

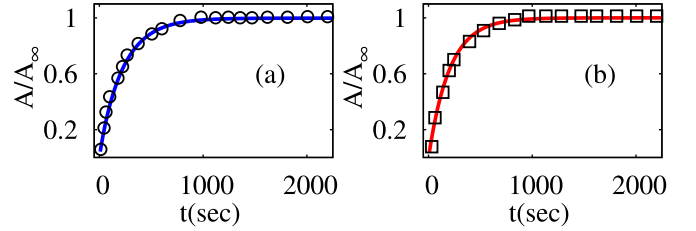


FIG. 4: Absorbance A versus time t , in sec. y-axis is scaled with the saturation value of absorbance $A_\infty = A(t \rightarrow \infty)$. The symbols in the left and the right figures are experimental data for $\rho_0 = 0.001 \text{ mg/ml}$ and $\rho_0 = 0.1 \text{ mg/ml}$, respectively. The solid lines are results from our numerical integration. We predicted the values of ω_b, ω_u by asking for what values of these parameters the integration results matches with both these data sets well. For this plots these we took $N_s = 2N_0$. But we checked robustness of these values of ω_b and ω_u at $N_s = 5N_0$ also.

The two panels of Fig.4 show fits to the experimental data which differs only in the antigen density ρ_0 . We use $D = 1.2 \times 10^{-5} \text{ cm}^2/\text{sec}$ for the diffusion constant, typical of diffusion of small molecules in water[12, 13] and assumed $N_s = 2N_0$, which fixes σ_0 . The reasonably good fit was obtained by choosing the following values for the kinetic coefficients: $\omega_b = 4.9 \times 10^{-4} \mu\text{m}^3/\text{sec}$ and $\omega_u = 5.0 \times 10^{-3}/\text{sec}$. Similar ball park numbers were used in Ref[11] for surface reactions on bacterial membrane. Using this model one can get a good estimation about D, ω_b, ω_u provided the N_s/N_0 ratio is known.

For the rest of our discussion we will be using these values of ω_b, ω_u , and D obtained above, and we will keep ρ_0 fixed at 0.1 mg/ml . Given the nature of the A versus t curve, we

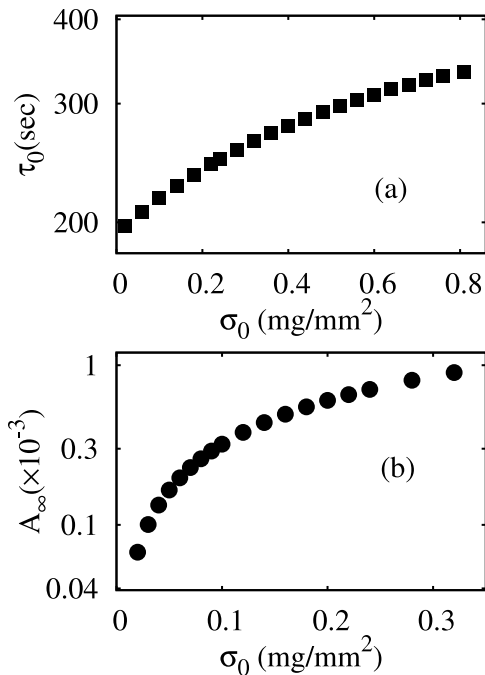


FIG. 5: Semi-log plots of, (a) the saturation time (τ_0) versus σ_0 , the surface density of antibody and (b) maximum absorbance A_∞ versus σ_0 . These are obtained from our numerical integration, keeping the value of $\rho_0 = 0.1 \text{ mg/ml}$ fixed. The values of ω_b and ω_u are same as those found through Fig.4. Here σ_0 is varied over a range such that N_s/N_0 correspond to a range [1, 30] for (a) and [1, 12] for (b). This dominance of antibody was chosen so that most of the antigens in the bulk get absorbed, as we learned from Fig.3. It is clear from (b) that $N_s/N_0 \sim 10$ (which here corresponds to $\sigma_0 \sim 0.3 \text{ mg}/\text{mm}^2$) is optimum for maximising the absorbance without significant increase in τ_0 (see 5(a)). Here we calculated A from σ using the parameter values $\varepsilon = 21 \times 10^4 \text{ M}^{-1} \text{ C m}^{-1}$, $N_A = 0.37$, $\delta = 1 \text{ nm}$, and $\lambda = 280 \text{ nm}$ [8].

fit it to the approximate formula $A(t) = A_\infty(1 - \exp^{-t/\tau_0})$, in order to estimate the saturation time τ_0 , shown in Fig.5(a) and Fig.6(a). The saturation value, defined as $A_\infty = A(t \rightarrow \infty)$ is shown in Fig.5(b) and Fig.6(b). Note that both τ_0 and A_∞ are functions of σ_0 and ρ_0 . Since $\sigma_0 \propto N_s$ and $\rho_0 \propto N_0$, their ratio is proportional to N_s/N_0 which serves as a convenient measure for the relative strengths of the reactants in the system, although the physics depends on N_0 and N_s both, and not only on N_s/N_0 .

Fig.5 shows that at fixed ρ_0 absorbance (A_∞) can be maximised by increasing N_s , because absorbance rate is proportional to $(\sigma_0 - \sigma)$. Although this comes at the cost of higher waiting time (τ_0), note that the increase in absorbance is relatively much higher compared to the increase in the waiting time (less than two times). Therefore it is worth the wait. As explained in the caption, we infer that $N_s/N_0 \sim 10$ is the optimum ratio when absorbance can be maximised without a significant increase in waiting time. But in practical situation, since one would not know N_0 a priori, it is always beneficial to start with a high antibody concentration for efficient capture

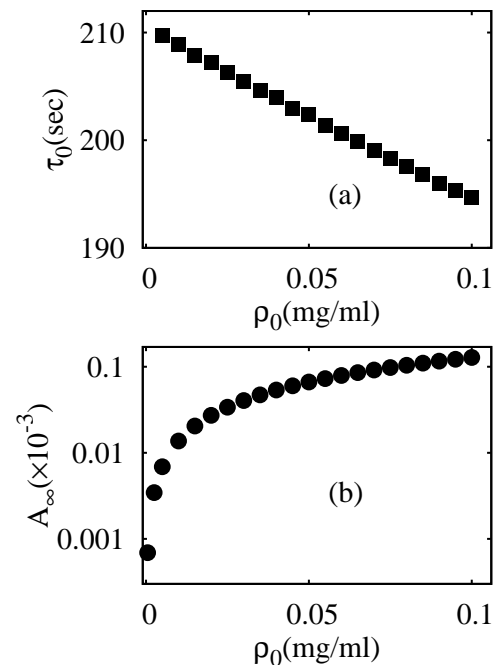


FIG. 6: (a) Saturation time τ_0 versus ρ_0 , the injected antigen concentration, and (b) Semi-log plot of maximum absorbance A_∞ versus ρ_0 . These plots are obtained at a fixed value of σ_0 , while values of ω_b and ω_u are same as those found through Fig.4. These plots focus on the utility of the sensor at low ρ_0 concentration. Therefore ρ_0 is varied in a range such that $N_0/N_s \leq 1$, and the maximum of ρ_0 corresponds to $N_0 = N_s$. (b) shows that absorbance drops drastically at very low ρ_0 concentration (where $N_0/N_s \leq 1/4$). However in (a) τ_0 changes little over the whole range.

of antigens. Also note that comparison between Fig.3(a) and Fig.3(c) also gives the same message that at higher N_s/N_0 antigen capture is maximal, leading to diminished antigen concentration left in the bulk.

Fig.6, as mentioned in its caption focus on the utility of the sensor at low ρ_0 concentration. It shows that for a fixed σ_0 the waiting time τ_0 goes up as ρ_0 goes down, i.e., lower concentration of antigens take a longer time for the absorbance to saturate. This may appear counter intuitive, but this is because the binding slows down if ρ is less (see Eq.4). However this slow down being very small (in the range 190-210 sec) is not the real concern, instead the absorbance which reduces by an order of magnitude at $N_0/N_s \leq 1/4$, limits the utility of the sensor at low ρ_0 (see Fig.6b).

Our discussion so far focused on the sensitivity of a sensor at low concentration of antigens. Another practical question could be for what range of concentrations a sensor can show significant absorbance within a given time (typically minutes). Towards this one studies the absorbance at fixed time as a function of ρ_0 , for a fixed σ_0 . Both, our mean field analysis and numerical solution of the coupled PDE (see Fig.7), show that at a fixed time absorbance varies linearly with ρ_0 in the low ρ_0 regime and non linearly at the high ρ_0 regime. Fig.7a

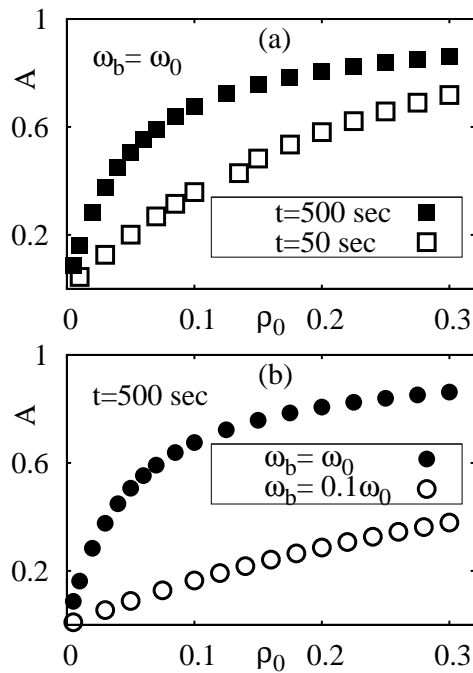


FIG. 7: (a) A versus ρ_0 at time ($t = 50, 500$ sec), keeping ω_b constant, (b) A versus ρ_0 at binding constant ($\omega_b = \omega_0, 0.1\omega_0$), for a fixed time.

shows that at early times absorbance remains linear with respect to ρ_0 , up to a wider range of ρ_0 . Fig.7b shows even at late times ($t = 500$ sec) a wider linear regime may result from a lower value of ω_b , although ω_b is not a tunable parameter for a given system.

In summary, our detailed study of the spatio-temporal behaviour of the sensor reveals that in certain parameter regime, where the diffusion time scale is fastest among all the relevant time scales of the system, an analytic mean field solution is possible. We also identified the optimum value of the antibody concentration σ_0 (corresponding to $N_s/N_0 \sim 10$) such that further increase of σ_0 does not lead to any significant improvement in detection efficiency. It is somewhat counter-intuitive that higher σ_0 also results in higher saturation time

which is not beneficial for quick detection capability. We note that the ratio N_s/N_0 solely does not determine the behaviour but both N_s, N_0 (equivalently σ_0, ρ_0) are individually important. Although possible effect of nonspecific binding on the functionalised surface can be easily included in our theoretical model, we ignored it here because for the particular chemical system we considered here, experimentally the effect turned out to be negligible. To check this, absorbance was measured for a chamber filled with water only (i.e., no antigens). Further, possibility of second order surface reactions can also be included in our model, although analytic mean field solutions are difficult for higher order surface reaction. Other subtle effects resulting from the cooperativity in binding have been considered recently for dendrimers [14].

-
- [1] Tao Geng, Joe Uknalis, Su-I Tu and Arun K. Bhunia, *Sensors* **6**(8), 796 (2006).
 - [2] Sheng Wu, Zhaoyang Zhong, Dong Wang, Mengxia Li, Yi Qing, Nan Dai and Zengpeng, *Microchim Acta* **166**, 269 (2009)
 - [3] Sara Rodriguez-Mozaz, M. P. Marco, M. J. L. De Alda, and D. Barcelo, *Pure Appl. Chem.* **76**, 723 (2004)
 - [4] D.R. Thevenot, K. Toth, R.A. Durst, and G.S. Wilason, *Pure Appl. Chem.* **71**, 2333 (1999)
 - [5] M.D. Marazuela, M.C. Moreno-Bondi *Anal Bioanal Chem* **372** 664682 (2002)
 - [6] A. Sadana, D. Sii *Biosensors and Bioelectronics*, 7 (1992)
 - [7] George P. Anderson *et.al. IEEE Engineering in Medicine and Biology* **739**, 5175 (1994)
 - [8] V. V. R. Sai *et.al.*, *Sensors and Actuators: Chemical B* **143**, 724 (2010)
 - [9] R. Narayanaswamy, *Acta Biologica Szegediensis* **50**, 105 (2006).
 - [10] V. Ruddy, B.D. McGrath, J.A. Murphy, *J. Appl. Phys.* **67**(10), 6070 (1990).
 - [11] K.C. Huang, Y. Meir, N.S. Wingreen *Proc. Natl. Acad. Sci. U.S.A.* **100**, 12724 (2003).
 - [12] Richard W. Pastort and Martin Karplus *J. Phys. Chem.* **92**, 2636 (1988)
 - [13] Douglas Brune, Sangtae Kim *Proc. Natl. Acad. Sci. U.S.A.* **90**, 3835 (1993).
 - [14] N.A. Licata and A.V. Tkachenko, *Phys. Rev. Lett.* **100**, 158102, (2008).